

Determination of the Energy Distribution of Bremsstrahlung from 19.5-Mev Electrons*

H. W. KOCH** AND R. E. CARTER***

Physics Department, University of Illinois, Urbana, Illinois

(Received September 23, 1949)

The conventional target of a 22-Mev betatron has been replaced by a 0.005-in. platinum target and the intensity spectrum of x-rays produced in the platinum by betatron-accelerated electrons has been measured. The kinetic energy of the monoenergetic electrons at the time of expansion was 19.5 Mev. The x-rays were collimated and observed in the forward direction by studying the electron-positron pairs produced in a cloud chamber filled with air. About 1300 pairs were measured. The intensity spectrum of x-rays is calculated from the pair energy distribution and is compared with the bremsstrahlung theory of Bethe and Heitler. The experimental intensity in the region of 10 Mev is found to be higher than the theoretical value by an amount which is larger than the statistical uncertainty of the experiment. Some details of the pair production process are given, and methods of correcting for instrumental discrimination are discussed and applied.

INTRODUCTION

THE non-relativistic wave-mechanical treatment of bremsstrahlung production has been developed in detail by Sommerfeld,¹ Sommerfeld and Maue,² and Weinstock.³ The theory was confirmed by the experiments of Nicholas,⁴ Kulenkampff,⁵ and Harworth and Kirkpatrick.⁶ There was agreement on the existence of a finite number of quanta at the high energy end of the spectrum produced by monoenergetic electrons impinging on a thin target.

In 1934, Bethe and Heitler⁷ developed a theory of bremsstrahlung which should be valid for electrons in the relativistic region. In addition, this theory gave the cross section for electron-positron pair production. The theory has been carried out only to the extent of the Born approximation and the validity of its predictions are thus limited. The theory has not been compared with a direct detailed experiment in the past, although some parts of it have been investigated. In particular, Lanzl, Laughlin, and Skaggs⁸ have shown that the ratio of the bremsstrahlung production cross sections for tantalum and copper was larger than the theoretical Z^2 factor by about eight percent for quanta having energies between 10.9 and 16 Mev.

The form of the theory which described the cross section for pair production has been investigated in the work of Adams,⁹ of Lawson,¹⁰ and of Walker¹¹ on x-ray absorption coefficients. They found discrepancies with the theory for high Z absorbers, and ascribed these to

the part of the absorption which resulted in the production of pairs.

A partial but more direct examination of the bremsstrahlung spectrum theory at energies of the order of 2 Mev was reported by Miller and Waldman.¹² They determined the spectral distribution at the high energy x-ray end and found a finite and constant intensity of radiation within several hundred kilovolts of the upper energy tip. Their experiment differed from the present one in that they had a monochromatic detector, and varied the electron energy. The result of the experiment was predicted by Guth,¹³ who used the Bethe-Heitler theory and applied a correction which was intended to remove the error due to the Born approximation.

Two reports have been published on previous determinations of betatron x-ray spectra, which are similar in principle to the present work. The first¹⁴ was the investigation of the Compton recoil electrons produced in a carbon radiator in a cloud chamber by the x-rays from a 2.8-Mev betatron. The intensity spectrum obtained by these authors is very different from that predicted.

The second spectrum experiment,¹⁵ which was done with a 20-Mev betatron, involved the two energy distribution determinations of the electron-positron pairs from a lead foil in a cloud chamber and the photo-protons in deuterium-loaded emulsions. The authors point out that unfortunately their measured spectrum "is not the spectrum that would be obtained if only the target radiation were measured."

Therefore, neither of the two reports permits a conclusive test of the Bethe-Heitler theory when it is applied to the radiation from 19.5-Mev electrons.

Several other methods have been proposed for the determination of betatron x-ray spectra by Baldwin and Klaiber,¹⁶ and by Lawson.¹⁷

¹² W. C. Miller and B. Waldman, *Phys. Rev.* **75**, 425 (1949).

¹³ E. Guth, *Phys. Rev.* **59**, 325 (1941).

¹⁴ W. B. Lasich and L. Riddiford, *J. Sci. Inst.* **24**, 177 (1947).

¹⁵ Bosley, Craggs, Nash, and Payne, *Nature* **161**, 1022 (1948).

¹⁶ G. C. Baldwin and G. S. Klaiber, *Phys. Rev.* **71**, 554 (1947).

¹⁷ J. L. Lawson *et al.*, ONR Quarterly Progress Report, General Electric Company (September, 1948).

* Assisted by the Joint Program of the ONR and the AEC.

** Present address: X-Ray Section, National Bureau of Standards, Washington, D.C.

*** Present address: Los Alamos Scientific Laboratory, Los Alamos, New Mexico.

¹ A. Sommerfeld, *Ann. d. Physik* **11**, 257 (1931).

² A. Sommerfeld and A. W. Maue, *Ann. d. Physik* **23**, 589 (1935).

³ R. Weinstock, *Phys. Rev.* **61**, 584 (1942); **64**, 276 (1943).

⁴ W. W. Nicholas, *Bur. Stand. J. Research* **2**, 837 (1929).

⁵ H. Kulenkampff, *Handbuch der Physik* (1933), Vol. 23, p. 2.

⁶ K. Harworth and P. Kirkpatrick, *Phys. Rev.* **62**, 334 (1942).

⁷ H. Bethe and W. Heitler, *Proc. Roy. Soc.* **146**, 83 (1934).

⁸ Lanzl, Laughlin, and Skaggs, *Phys. Rev.* **74**, 1261 (1948).

⁹ G. D. Adams, *Phys. Rev.* **74**, 1707 (1948).

¹⁰ J. L. Lawson, *Phys. Rev.* **75**, 433 (1949).

¹¹ R. Walker, *Phys. Rev.* **76**, 527 (1949).

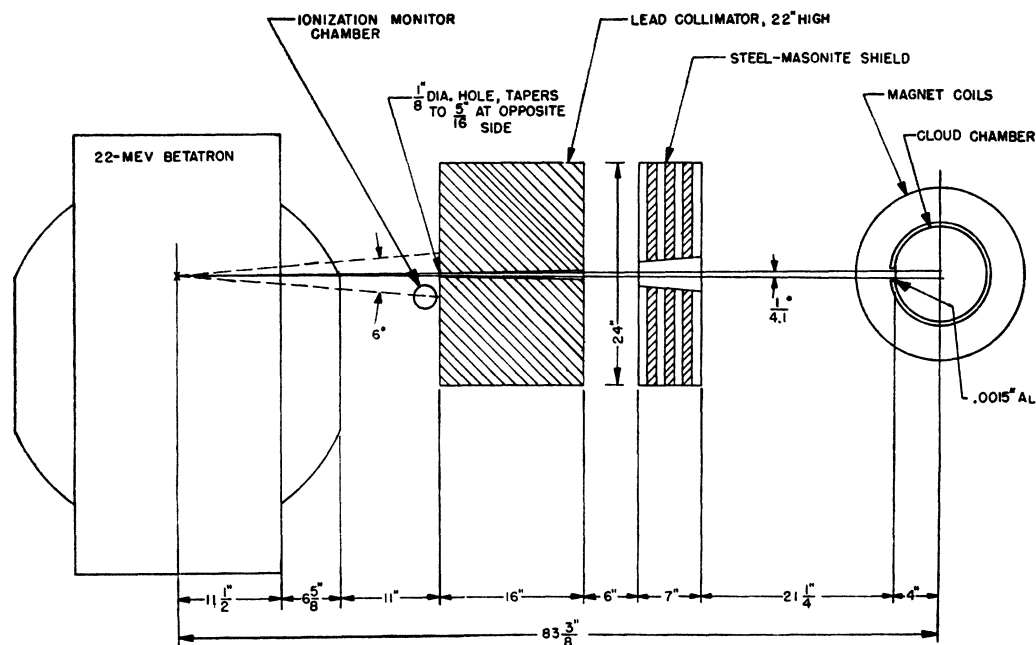


FIG. 1. Schematic diagram of the experimental arrangement.

The present experiment¹⁸ determined the energy distribution of bremsstrahlung, which was produced in a thin target of platinum by electrons accelerated in a 22-Mev betatron.¹⁹ Pair electrons were created in the gas of a cloud chamber by the betatron x-rays. The x-ray intensity distribution was calculated from the pair energy distribution, which was measured.

The principal purpose of the experiment was to obtain a set of experimental data which could be compared with the predictions of the Bethe-Heitler bremsstrahlung theory. The betatron is obviously ideal as a source of x-rays, because it produces a monoenergetic beam of high energy electrons. However, other requirements also had to be satisfied in order to permit a valid

test of the theory by the experiment. The following were regarded as essential in the present work:

- (1) The x-ray target was thin.
- (2) The x-rays were finely collimated so that only quanta, originating in the target and going in the forward direction from the target, entered the cloud chamber through a thin window.
- (3) The electron-positron pairs were produced in a low Z gas, so that the use of the theoretical pair production cross section would permit the accurate conversion of the pair energy distribution into the x-ray intensity distribution.
- (4) The pair particle characteristics were examined in detail experimentally, in order to make a rough test of the theoretical description of the pair production process and also to eliminate instrumental discrimination against certain energy groups of pairs.

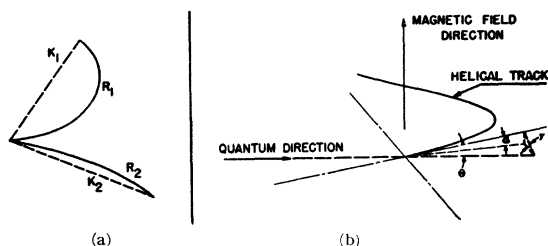


FIG. 2. Schematic drawing showing typical pair tracks. (a) Re-projection onto horizontal plane, in which the quantities measured were: (1) X - Y coordinates of pair origin; (2) conically projected radius, R ; (3) chord length, K , of particle arc with measured R . (b) Re-projection into three dimensions in which the quantities measured were: (1) Z coordinate of pair origin; (2) dip angle of particle helix, α ; (3) angle, θ , of particle with respect to quantum direction.

¹⁸ Preliminary reports have been given in Koch, Carter, and Robinson, Phys. Rev. 75, 172A (1949); and H. W. Koch and R. E. Carter, Phys. Rev. 75, 1950 (1949).

¹⁹ D. W. Kerst, Rev. Sci. Inst. 13, 387 (1942).

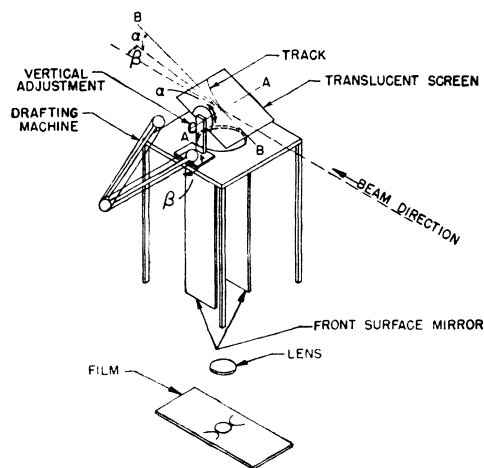


FIG. 3. Schematic drawing showing the apparatus used in the three-dimensional analysis of tracks.

It must be emphasized that an intensity spectrum result can only be applied to experiments in which a similar experimental arrangement is used. For example, the result in this paper is not applicable to an uncollimated beam of betatron x-rays emanating from a conventionally thick target.

APPARATUS

The experimental apparatus can be described in two parts: (1) The equipment required to produce a collimated beam of x-rays from the 22-Mev betatron; and (2) the equipment required to detect, photograph, and analyze the pair electrons.

1. The X-Ray Source

Figure 1 shows schematically the cloud-chamber arrangement in front of the 22-Mev betatron. The betatron was pulse-operated²⁰ so as to produce electrons with a kinetic energy of 19.5 Mev. The electron energy was accurately determined by the energy control built by Mr. H. Palevsky and described in principle in previous papers.²¹

After acceleration to the peak energy, the electrons bombarded a platinum target ($Z=78$), which was 0.005 in. thick. Electrons with energies of 19.5 Mev will lose approximately $\frac{1}{2}$ Mev energy due to ionization loss in going through the target. Therefore, the x-radiation produced by the electron bombardment of the platinum is considered thin target radiation.

The target was a relatively large flag, $\frac{3}{16}$ by $\frac{1}{4}$ by 0.005 in. thick, in order to insure that the x-rays being studied in the cloud chamber of Fig. 1 were emanating from the platinum target and not from other parts of the betatron vacuum chamber. The target projected out from the injector structure $\frac{3}{16}$ in. in the direction of the electron orbit. No obvious reduction in the x-ray intensity was observed as compared to that obtained from standard thicker targets.

The target thickness was tested by determining the total angle of the x-ray cone. Copper foils placed normal to the x-ray beam direction were used and the total angle of the half-intensity value of the copper activity was 6° for a betatron energy of 19.5 Mev. To within experimental error this is in good agreement with the

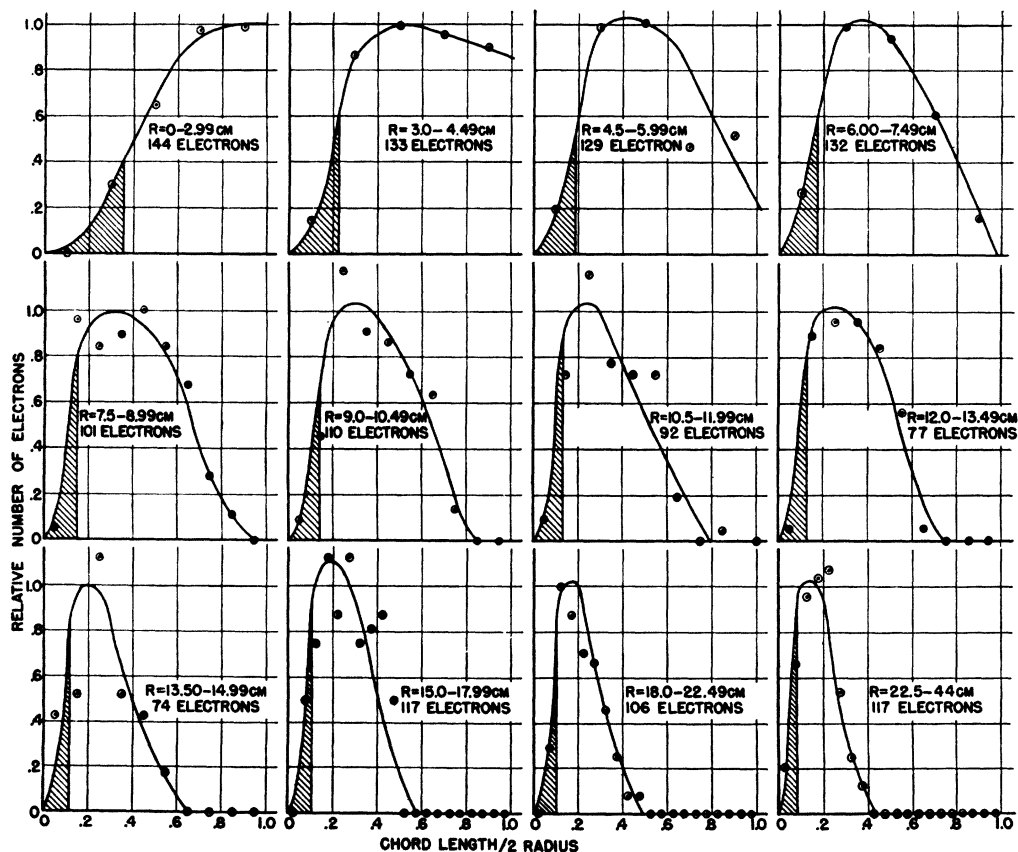


FIG. 4. Relative number of electrons whose radii of curvature fall within a certain interval, plotted as a function of chord length/2 radius. This is shown for several intervals of radius. The vertical line defining the right side of the shaded area in each plot corresponds to the minimum length of chord which was acceptable. All tracks falling in the shaded areas were discarded.

²⁰ H. W. Koch and C. S. Robinson, Rev. Sci. Inst. 19, 37 (1948).

²¹ See McElhinney, Hanson, Becker, Duffield, and Diven, Phys. Rev. 75, 542 (1949).

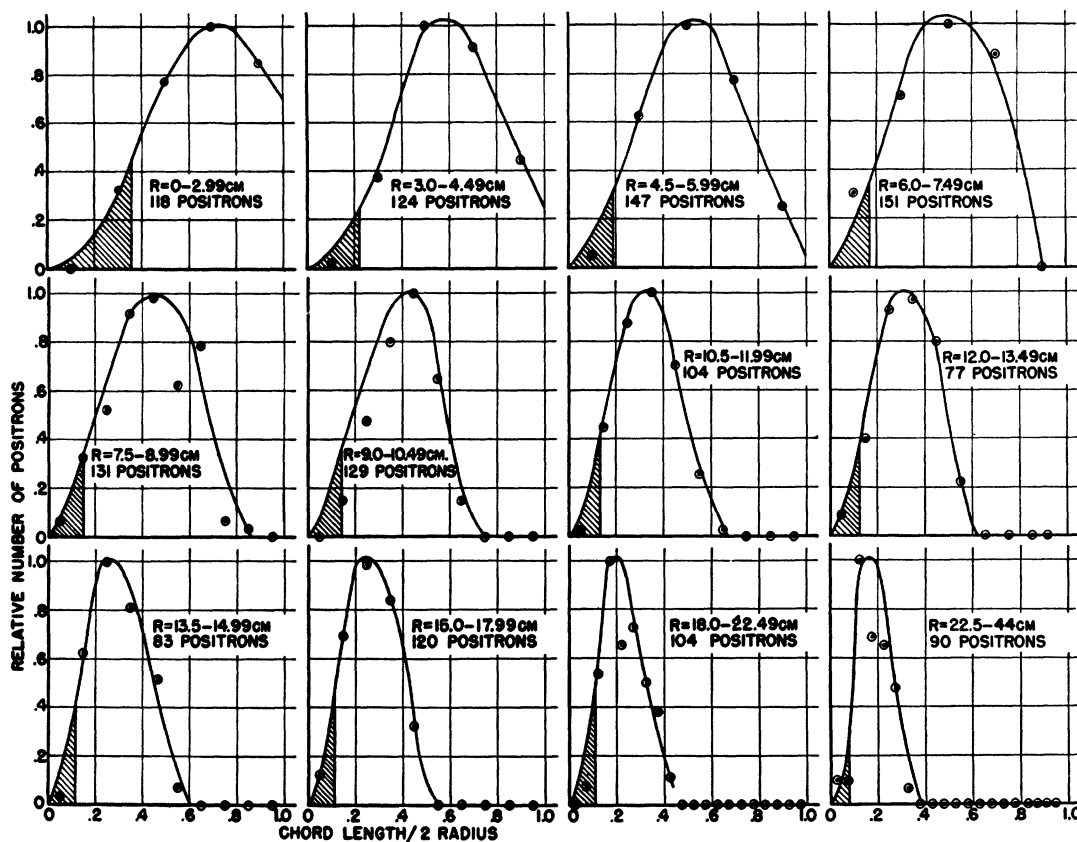


FIG. 5. Relative number of positrons whose radii of curvature fall within a certain interval, plotted as a function of chord length/2 radius. This is shown for several intervals of radius. The vertical line defining the right side of the shaded area in each plot corresponds to the minimum length of chord which was acceptable. All tracks falling in the shaded areas were discarded.

value predicted by Schiff²² for a 0.005-in. thick tungsten target.

Tests were also made on the focal spot size and the time duration of the x-ray burst. The focal spot size was measured by the use of a pinhole camera at several electron energy values. The spot size was 1.3 mm high

by 0.3 mm wide. No other images were observed. Therefore, it is believed that only the platinum target was serving as a source of x-rays.

The x-ray burst time width was examined by means of a 931 photo-multiplier tube plus a fast amplifier circuit. Mr. G. W. Rodeback built the circuits and showed that the x-ray burst for 19.5-Mev electrons was

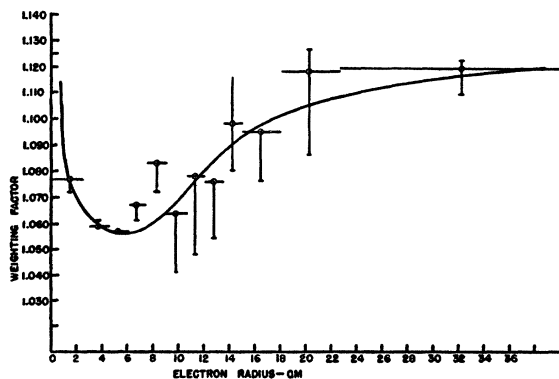


FIG. 6. Chord length weighting factor calculated for electrons to correct for effects of discrimination.

²² L. I. Schiff, Phys. Rev. 70, 87 (1946).

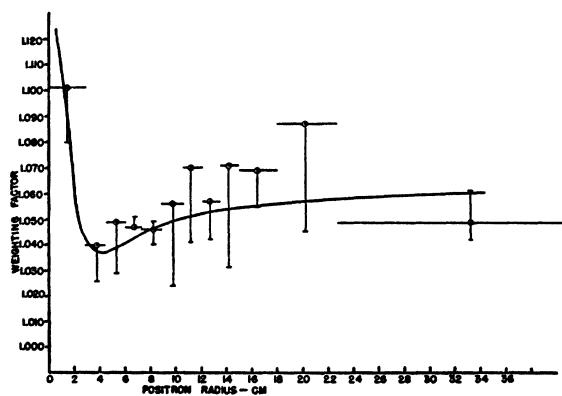


FIG. 7. Chord length weighting factor calculated for positrons to correct for effects of discrimination.

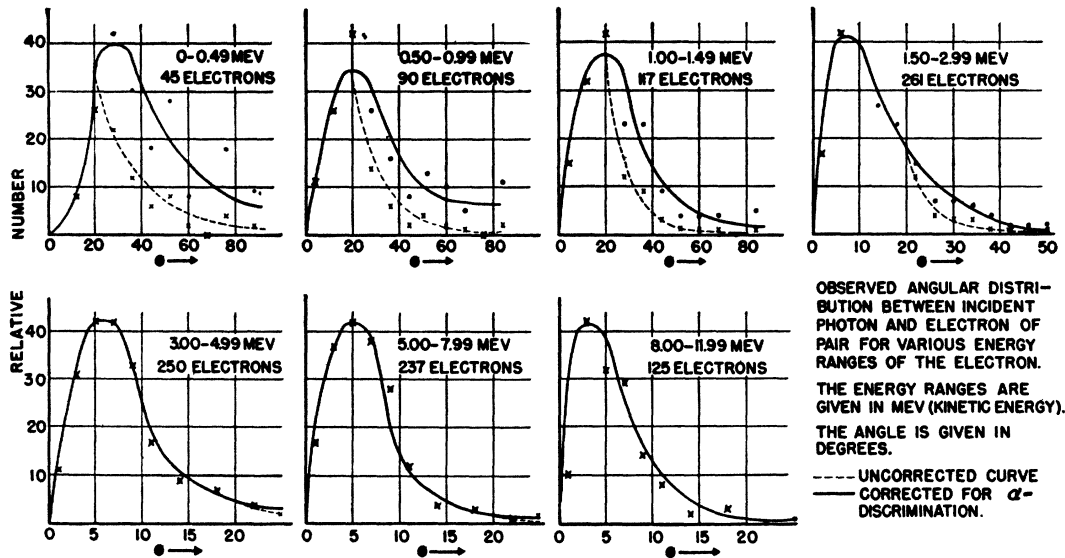


FIG. 8. Relative number of electrons in certain energy intervals plotted as a function of the angle (θ) they made with respect to the incident quantum.

a single burst and not a multiple burst as found previously²³ at one other energy.

Integral x-ray intensity measurements were made for each x-ray burst by means of a high pressure argon-filled ionization chamber and a charge integrating circuit.²⁴ The integrator readings were recorded on an Esterline-Angus recorder, which permitted the monitoring of the x-ray yield from the betatron during the entire period of the cloud-chamber exposures. The yield at the chamber position was approximately 1.9×10^{-6} R per

pulse as measured with a thick-walled ionization chamber. The argon chamber monitor was located between the betatron and the x-ray collimator as shown in Fig. 1.

The x-rays from the platinum target pass through a $\frac{3}{8}$ -in. thick wall of procelain before reaching the collimator, which consisted of a 16-in. thick lead wall (Fig. 1). The x-rays were collimated by means of the tapered hole in the lead, whose defining aperture for the betatron x-rays was $\frac{1}{8}$ in. in diameter at the entrance

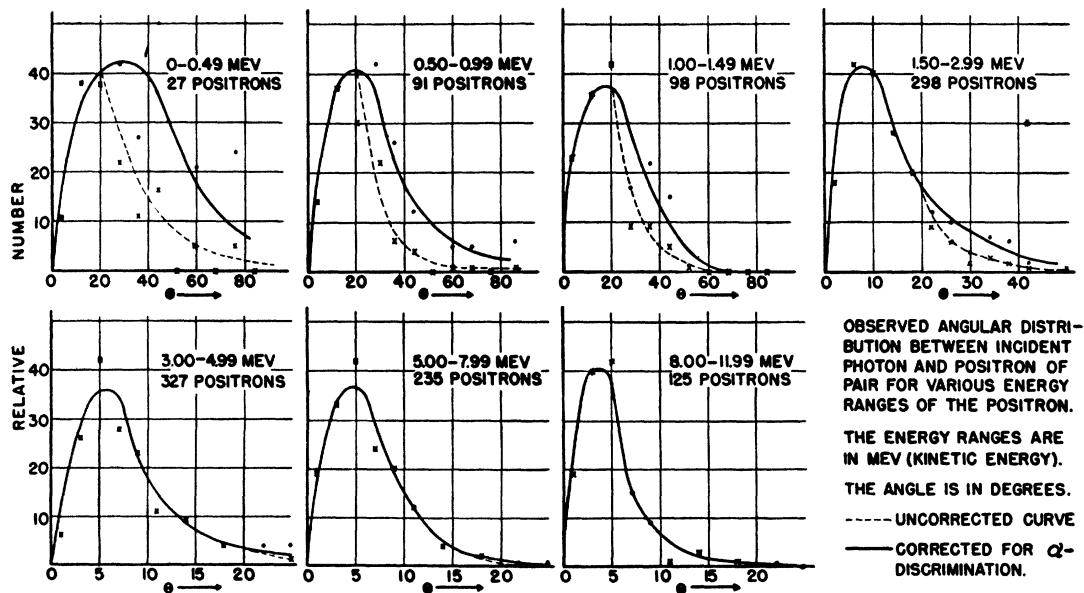


FIG. 9. Relative number of positrons in certain energy intervals plotted as a function of the angle (θ) they made with respect to the incident quantum.

²³ D. W. Kerst and H. W. Koch, Rev. Sci. Inst. 18, 681 (1947).

²⁴ J. S. Allen and D. E. Hudson, A.E.C.D. 2052, L.A.D.C. 232 (May, 1945).

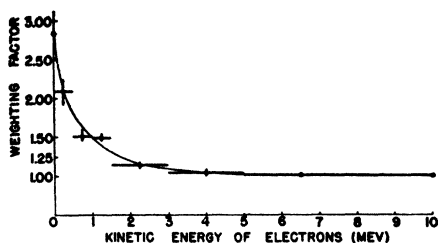


FIG. 10. Weighting factor necessary to correct for discrimination against electron tracks because of the selection criterion on the angle α .

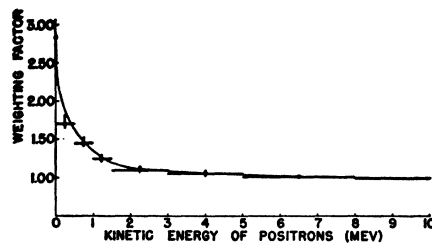


FIG. 11. Weighting factor necessary to correct for discrimination against positron tracks because of the selection criterion on the angle α .

end of the collimator. The primary beam so collimated was a cone whose whole angle was 0.24° . Since the exit aperture of the hole was $\frac{5}{16}$ in. in diameter, the secondary rays produced in the entrance end of the collimator were confined to a cone whose whole angle was 1.6° . Thus the collimator served two functions:

1. It insured that the x-rays that entered the cloud chamber were x-rays that came from the thin betatron target;
2. It reduced the number of secondary collimator rays that enter the cloud chamber. It also permitted an evaluation of the number of secondaries as indicated in the discussion section.

2. Detection, Photography, and Analysis of Pairs

Pair electrons were produced in the gas of the cloud chamber by the betatron x-rays. The gas consisted of 1.4 atmos. of air saturated with a three to one ratio of ethyl alcohol and water vapor. The temperature regulated chamber was 8 in. in diameter and 1.5 in. deep with an illuminated region $\frac{1}{2}$ in. high. The x-rays at the chamber position were confined to an approximate cylinder whose diameter was $\frac{3}{8}$ in. and which was located centrally in the illuminated region. The beam was admitted to the chamber through a 0.0015-in. Duralumin window in order to increase the ratio of pair electrons produced in the gas to background electrons from the wall.

The chamber magnetic field was pulsed on for 1.5 sec. once every 30 sec. by the field control circuit of a 25-kw motor generator set. The chamber field current was kept constant at 59.0 (± 0.2) amp. at the time that the x-ray burst entered the cloud chamber. The field intensity corresponding to this current value was 1540 gauss as calibrated by means of the proton magnetic field detector similar to that described by Roberts.²⁵ The field was constant within the illuminated volume of the chamber to ± 0.3 percent.²⁶

Synchronized with the x-ray burst, which bombarded the cloud chamber once every 30 sec., were the shutters of two mercury arc lamps and of a specially built 35-mm camera. The lamps were GE H-6 lamps and the camera lens was a Kodak Eklar $f/1.9$ lens, 50-mm focal length, which was operated at $f/3.5$ in order to obtain sufficient

depth of field. Forty thousand stereoscopic pictures were taken during a three-week period.

After the pictures were taken and the film was developed in D-11 developer, the film was examined, either by replacing and reprojecting the film in the original camera-mirror system to produce three-dimensional pictures of the pairs photographed, or by reprojecting the film on to a horizontal plane. Both methods were used to examine 10,300 of the frames. The analysis procedure is schematically described in Fig. 2.

The tracks in the horizontal plane projection are helices which are conically projected by the optics of the original camera system. The principal quantity measured is R , the average radius of the arc whose chord length was also measured. The chord lengths are limited by multiple scattering, by the tracks going out of the lighted region, and by the tracks going out through the walls of the cloud chamber. The classification of a chord length into one of these three categories was recorded. In addition, the x and y coordinates of the origin of the pair as well as quantities describing the accuracy of the measurements were noted.

In order to describe fully the electrons and positrons in space, the related angles had to be measured. These were obtained from the three-dimensional reprojection system described in Fig. 2(b). The quantities measured are α , which determines the component of momentum being acted on by the magnetic field, and β , which together with α , describes the angle θ between the outgoing electron or positron and the incoming quantum.

Figure 3 shows the three-dimensional analysis arrangement which is similar to that used by Brueckner, Hartsough, Hayward, and Powell.²⁷

In the selection of tracks to be measured and in their measurement, certain selection criteria were applied to insure that all particle energies used in the final data have a probable error less than a given tolerable maximum. The selection criteria center around the values of α and R and could conceivably produce a marked discrimination against certain energy ranges of pairs.

In the case of the radius, R , the selection criterion arises from the fact that the length of the arc determines

²⁵ A. Roberts, Rev. Sci. Inst. 18, 845 (1947).

²⁶ H. W. Koch, J. Exp. Phys. (to be published).

²⁷ Brueckner, Hartsough, Hayward, and Powell, Phys. Rev. 75, 555 (1949).

the accuracy with which an arc of a given radius of curvature can be measured. The radius of curvature of a track was measured by a comparison of the arc with standard arcs scribed on a thin sheet of Lucite. This type of comparison is based on the observer being able to detect a difference ΔS in the sagitta for the arc being measured and the standard curve. Since the sagitta is related to the radius and the chord length, K , by the equation

$$S = K^2/8R, \quad (1)$$

the differential form for a given K becomes

$$K^2 = 8R\Delta S/(\Delta R/R). \quad (2)$$

An experiment on known arcs was made with several observers to determine the error in R , $(\Delta R/R)$, as a function of chord length and radius. It was found that ΔS could be determined and was approximately a constant. From these results, it was possible to fix the minimum chord length required for a given radius in order to insure that the probable error in the measured radius would be five percent. The chord length criterion that was used in the selection or omission of pair components was

$$K_{min} = 0.978 \times R^{1/2}. \quad (3)$$

The application of this criterion might be expected to result in discarding more tracks in one energy region than in another. In order to look for such discrimination, the relative number of tracks having radii of curvature within a certain interval was plotted as a function of chord length. This was done for several intervals of radii of curvature. Figure 4 contains such a plot for all electrons which were judged, by two or more observers, to be one of the components of a true pair. The same information concerning the positrons is contained in Fig. 5. For convenience, the abscissas are made $K/2R$, instead of simply K .

On both sets of curves the minimum acceptable values of $K/2R$ are indicated by the vertical line defining the right side of the shaded area. All tracks whose measurements caused them to fall in the shaded areas were discarded. In order to correct for the pairs which have been discarded due to the chord length

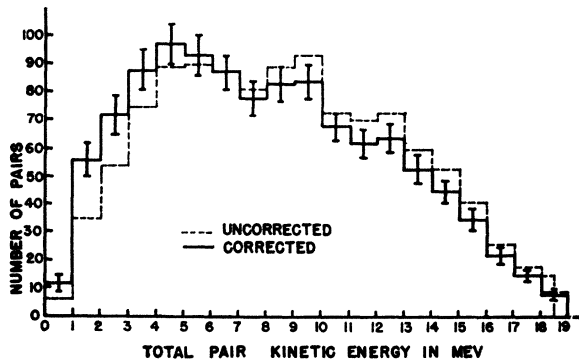


FIG. 12. Electron pair energy spectrum.

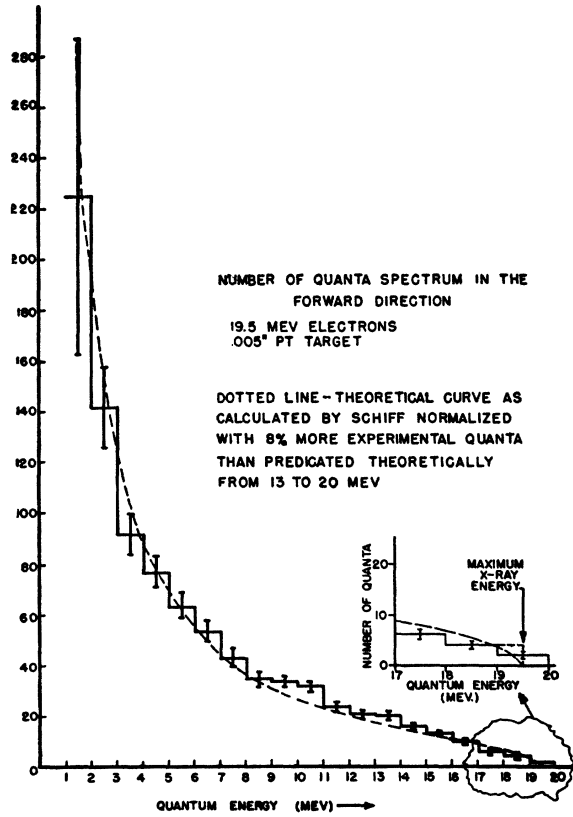


FIG. 13. Number of quanta as a function of energy, obtained by dividing the curve in Fig. 12 by the theoretical pair production cross section for air.

criterion applied to the electrons or positrons, a weighting factor has been calculated from the ratio of the total area of a given curve to the area representing those electrons that are kept for the final data. The weighting factors for electrons are therefore defined as

$$W \cdot F_E^K = (N_{SE}^K + N_{DE}^K)/N_{SE}^K, \quad (4)$$

where N_{SE}^K = number of electrons in the K sample, N_{DE}^K = number of electrons discarded from the K

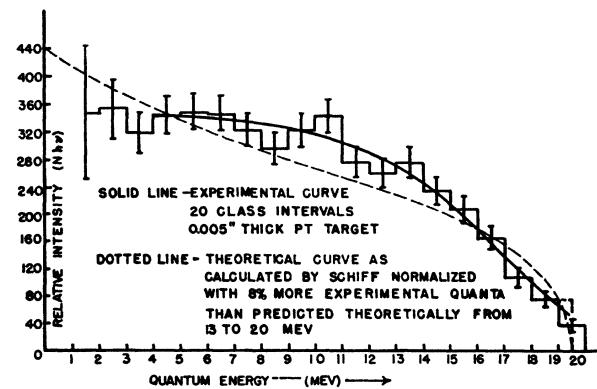


FIG. 14. Intensity spectrum in forward direction, 19.5-Mev electrons.

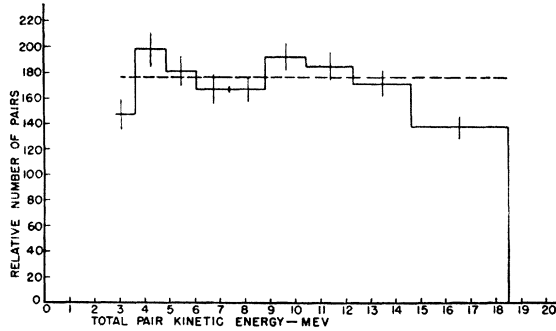


FIG. 15. Experimental electron pair spectrum with unequal energy intervals. For the width and position of the energy intervals as used, the theoretically predicted spectrum is rectangular in shape.

sample. A similar set of weighting factors was calculated for positrons. The chord length weighting factor has been plotted as a function of radius for electrons in Fig. 6 and for positrons in Fig. 7.

In the case of α , the dip angle of a track, the selection of allowable tracks depends upon the size of the angle. Since α is measured essentially by drawing a straight line from the track origin to a point further up the helical track the measured value is always greater than the true value and the error in the measurement increases with α . The selection criterion applied to the α -values was $-20^\circ \leq \alpha \leq +20^\circ$. Any particle whose absolute value of α was greater than 20° was discarded. More low energy pairs than high energy pairs were discarded due to the α -criterion on the individual electron tracks. In order to check the discrimination, the distributions of θ , the angle between the electron or positron and the incoming quantum were plotted. The dotted curves in Fig. 8 for electrons and in Fig. 9 for positrons represent the uncorrected data. The correction factor at any given value is obtained from the particular azimuthal angle, γ (see Fig. 2(b)), which is limited by the 20° α -criterion. All γ -angles are assumed equally probable. This is permissible unless the x-ray beam is polarized.

As in the case of the chord length distribution curves, weighting factors are calculated for electrons and for positrons as a function of the particle energies from the relative areas under the corrected and uncorrected curves of Figs. 8 and 9. The α -weighting factors for electrons are defined as

$$W.F.E^\alpha = (N_{SE}^\alpha + N_{DE}^\alpha) / N_{SE}^\alpha \quad (5)$$

and are plotted in Fig. 10 and for positrons in Fig. 11.

If the K discrimination is first applied to all the pairs and if the number of electrons or positrons is not greatly reduced at a given energy by α -discrimination, then it can be shown that the true number of pairs of a given total energy and of a given distribution in energy between positron and electron is given by

$$N_{TP} = N_{SP}^\alpha \{ 1 + [W.F.E^K + W.F.E^\alpha + W.F.P_0^K + W.F.P_0^\alpha - 4] \}. \quad (6)$$

N_{SP}^α is the number of pairs in the sample which have survived both the K and α -discriminations. N_{SP}^α is always equal to 1, since the pair weighting factor, N_{TP} / N_{SP}^α is applied to each individual pair.

As can be seen from a comparison of Figs. 6 and 7, and 10 and 11, the discrimination due to the α -selection criterion is more important than that due to the chord length criterion.

RESULTS

From the 10,300 pictures that have been analyzed, data were obtained on approximately 1300 pair electrons produced in the field of a nucleus and 33 pair electrons produced in the field of an electron. The principal purpose of the present experiment was to determine the x-ray spectral distribution when a thin platinum target is bombarded by monoenergetic electrons. Therefore, the details of the pair production and triplet production processes are presented here only to enlarge upon the x-ray spectrum interpretations.

The dotted histogram of Fig. 12 gives the distribution of 1122 pairs which survived the K and α -selection criteria. The solid histogram is corrected for the K and α -discriminations by applying the weighting factors of Figs. 6-11, to the individual pairs that were used to plot the uncorrected, dotted histogram. The abscissa scale is in terms of pair kinetic energy. Since the betatron for this experiment was operated so as to produce a peak x-ray energy of 19.5 Mev, the maximum obtainable pair energy was 18.5 Mev. Therefore, the number of pairs in the last 1-Mev interval of Fig. 12 should be doubled and the energy interval width should be plotted as a $\frac{1}{2}$ -Mev interval. This is indicated in Fig. 12 as a dark-dotted rectangular interval and is the procedure which will be followed in the subsequent x-ray energy distributions.

Since the pair electrons were produced in a low Z material, air, the pair production cross section given by Heitler²⁸ was assumed correct.²⁹ Dividing each ordinate

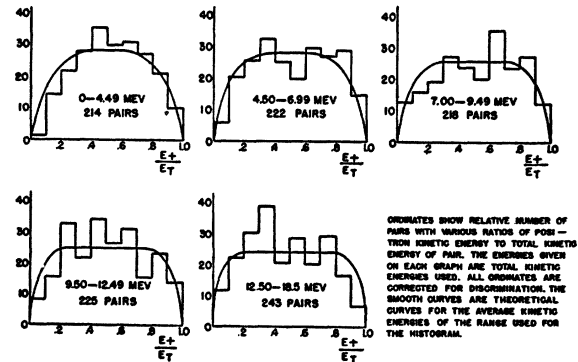


FIG. 16. Energy distribution of pairs.

²⁸ W. Heitler, *Quantum Theory of Radiation* (Oxford University Press, London, 1936), first edition, p. 200.

²⁹ See G. D. Adams, *Phys. Rev.* **74**, 1707 (1948); C. L. Cowan, *Phys. Rev.* **74**, 1841 (1948); and R. L. Walker, *Phys. Rev.* **76**, 527

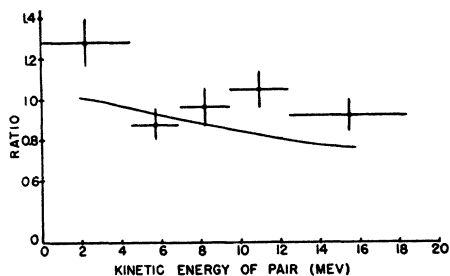


FIG. 17. Ratio of number of positrons with 0.3 to 0.7 of the total kinetic energy of the pair to remaining number of positrons.

on the corrected histogram of Fig. 12 by the corresponding pair production cross section gives the spectrum of quanta Fig. 13. A small correction has also been made for the x-ray absorption in the betatron vacuum chamber wall. The dotted line is the theoretically predicted intensity spectrum in the forward direction and for a thin platinum target as calculated by Schiff using the Bethe-Heitler theory.³⁰ The theoretical curve has been normalized by providing for eight percent more experimental quanta than are theoretically predicted from 13 to 20 Mev.³¹

A more conventional plot of the data is shown in the intensity plot of Fig. 14. The emphasis of the low energy end in the number of quanta spectrum is removed in the intensity spectrum. The most apparent difference in shape between the theoretical and experimental curves of Fig. 14 occurs near the middle energy ranges, where the experimental intensity is relatively higher than the theoretical curve at a quantum energy of 10 Mev. At the higher energy tip of the spectrum the statistics are too poor to state definitely that the intensity is constant for 1 Mev below the maximum energy, although the experimental points do not contradict such a statement. Because of the uncertainty, the solid curve of Fig. 14, which best represents the experiment, has not been drawn above 19.3 Mev.

The solid curve has also not been drawn for quantum energy values below 4 Mev. Below this energy the values are believed unreliable because the weighting factor principle for pairs is not valid when the probability for pairs being discarded becomes appreciable. This latter condition occurs below pair kinetic energies of 3 Mev.

Since the discrepancy between experiment and theory in the middle energy ranges of Fig. 14 depends on the normalization method used for the theoretical curve, the electron pair energy distribution has been replotted

(1949) for the latest results and the references in the literature. The theoretical pair production cross section for air is within three percent of the experimental value at energies between 10.9 and 18.7 Mev according to the results of the first reference.

³⁰ L. I. Schiff (private communication). See also reference 22.

³¹ The normalization procedure used in reference 18 provided for 10 percent more quanta experimentally than theoretically predicted between 12 and 20 Mev. The figures of eight percent and 13 to 20 Mev which are used in the present report are a more correct interpretation of the results given by Skaggs *et al.* in reference 8.

in Fig. 15, in order to permit an actual comparison of shapes independent of normalization. In this plot, the width and position of the energy intervals of Fig. 12 are selected so as to transform the theoretically predicted pair spectrum into a rectangular distribution. The best fitting theoretical curve, which is now a horizontal straight line, has been drawn between the energies of 3 and 18.5 Mev. Obviously, the theoretical shape does not best represent the experiment especially near the high energy tip. The conclusion drawn from the curves in Fig. 14, that the theoretical prediction is low in the middle energy region, would be consistent with Fig. 15.

The great advantage to the unequal width interval plot is the ease with which tests can be made of the adequacy of the experimental statistics. If the theory best represented the experiment, then the experimental points would fall within a band of the theoretical horizontal line. The band width above and below the line would be determined by the statistical accuracy of the points. In the present experiment, no straight line fits the experimental data. Therefore, the statistical accuracy of the experiment is sufficient to prove a discrepancy with the theory in the middle energy ranges.

Other tests have given the same indications. For example, the spectral distribution of pairs determined for the front half and for the back half of the cloud chamber were very similar in shape. Also, plots have been made using 30 energy intervals in place of the 20 1-Mev intervals used in Fig. 12 and again there are more pairs in the middle energy ranges than are predicted.

The results³² on the details of the pair and triplet production processes are given in Figs. 18 and 16-19.

The plots in Fig. 16 are frequency histograms of the ratio of the positron energy to the total pair energy for five ranges of the total pair energies. The theoretical fractional energy curves of Bethe and Heitler⁷ have been drawn on each histogram.

To test the relative shapes between the experimental and theoretical curves a calculation was made of the

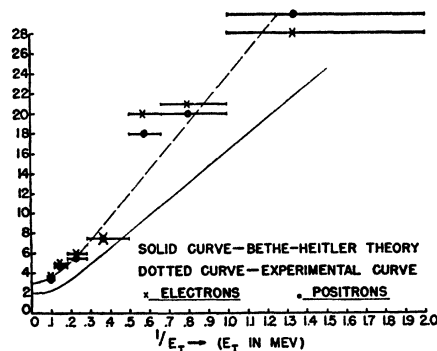


FIG. 18. Plot of θ_{\max} versus $1/E_L$.

³² A very complete report of similar results at an x-ray energy of 2.6 Mev is given in L. V. Groshev, J. Phys. U.S.S.R. 5, 115 (1941).

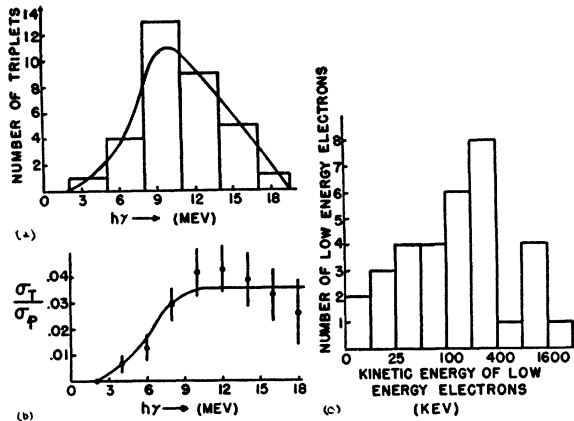


FIG. 19. Data for air concerning pair production in the field of an electron. (Data collected from 33 observed triplets.) (a) Energy distribution of the triplets. (b) Ratio of the triplet-to-pair production cross sections at a given quantum energy as obtained from Figs. 19(a) and 12. (c) Energy distribution of the low energy electrons of triplets. The minimum detectable energy was of the order of 10 kv.

ratio of the number of positrons with 0.3 to 0.7 of the total pair kinetic energy to the remaining number of positrons. The ratio has been plotted in Fig. 17. The smooth curve shows the theoretical ratios, which in general are lower than the experimental points.

According to Bethe and Heitler⁷ there should be an energy difference between the average positron energy and the average electron energy. The difference will be of the order of $2 mc^2 Z/137$ for small quantum energies; for higher $h\nu$ the difference will be smaller. Since $2 mc^2 Z/137$ is approximately 60 kv for a Z of 8, no difference could be determined in the present experiment. The experiment was thus not in disagreement with the prediction, since calculated values of \bar{E}_+/E_T and \bar{E}_-/E_T showed no detectable asymmetry in the positron and electron energies.

The distributions of the angle between the individual particle and the incoming quantum direction have already been presented in Figs. 8 and 9. A comparison with the theoretical expression³³

$$\theta^2 d\theta / (\theta_0^2 + \theta^2)^2 \ln \left\{ \frac{(\theta_0^2 + \theta^2)}{\theta_0^2} + B \right\}, \quad (7)$$

where $\theta_0 = mc^2/E_T$ and B is a constant, was made in Fig. 18 by plotting the angles of the maxima³⁴ of Figs. 8 and 9 as a function of the particle total energy. The θ_{\max} calculated from Eq. (7) is drawn as a smooth curve. The experimental values are all higher than the corresponding theoretical values.

The data on triplets are very poor statistically, since only 33 triplets were found in the pictures that con-

tained 1300 pairs. However, the little data on triplets is consistent and indicates that very few triplets could have been mistaken for pairs and included in the pair energy distribution of Fig. 12. A smooth curve best representing the data has been drawn on the triplet energy spectrum of Fig. 19(a). A division of the number of triplets on the smooth curve at a given quantum energy by the number of pairs found at the same energy results in the ratio of the triplet production to pair production cross sections. The cross-section ratios *versus* quantum energy are plotted in Fig. 19(b). The smooth curve has been drawn leveling off at energies above 10 Mev as would be expected from any of the triplet production theories.

The value for the cross-section ratio that Phillips and Kruger³⁵ found at 6.5 Mev was 0.035, which is not in disagreement with the ratio of 0.022 found in the present experiment (Fig. 19(b)).

Figure 19(c) is the frequency distribution of energy for the low energy electron of the 33 triplets. The histogram is plotted on a logarithmic energy scale and has a shape very similar to that found by Phillips and Kruger for their triplets. The shape is also similar to that found for the nuclear recoils produced by the pairs in the present experiment and discussed in the following paper.

DISCUSSION

The possible criticisms of the present work center around the effect of secondaries from the collimator and around the statistical uncertainties in the interpretation of an x-ray spectrum based on 1122 pairs.

It was pointed out in the discussion of the collimator that the secondary rays from the collimator were emitted into a cone whose angle was 1.6° as compared to the primary cone of angle 0.24° . The measurement of the X , Y , and Z coordinates of the pair origins showed that only four pairs were produced in the cloud-chamber external to the primary beam. These must have been produced by scattered quanta which did not come directly from the target. It was then calculated that not more than six pairs were formed in the region of the primary beam by other scattered secondary quanta, which are emitted from the collimator into a cone whose whole angle is greater than 6° .

The statistics in the present experiment are admittedly poor and should be improved. However, the conclusion that in the energy range from 8 to 12 Mev, the experimental number of quanta is relatively greater than the Bethe-Heitler prediction seems clear. This cannot be ascribed entirely to poor statistics.

The authors are indebted to Professors C. S. Robinson, A. T. Nordsieck, and D. W. Kerst for their invaluable suggestions and help. Mr. George Modesitt capably performed much of the tedious analysis.

³³ H. Bethe and W. Heitler, Proc. Camb. Phil. Soc. **30**, 559 (1934). See also the comments of J. C. Jaeger and H. R. Hulme, Nature **142**, 573 (1938).

³⁴ Some of the experimental average angles are given in the following paper by G. Modesitt and H. W. Koch, Phys. Rev. **77**, 177 (1950).

³⁵ J. Phillips and P. G. Kruger, Phys. Rev. **76**, 1471 (1949).